Optik 127 (2016) 1792–1796

Contents lists available at ScienceDirect

Optik

journal homepage: www.elsevier.de/ijleo

Synthesis and optical limiting properties of graphene oxide/bimetallic nanoparticles

Chan Zheng*, Wei Li, Xueqing Xiao, Xiaoyun Ye, Wenzhe Chen

College of Materials Science and Engineering, Fujian University of Technology, 3 Xuefu Road, Fuzhou 350108, PR China

ARTICLE INFO

Article history:
Received 5 August 2015
Accepted 12 November 2015

Keywords:
Graphene oxide
Metal nanoparticles
Optical limiting
Nonlinear optical
Z-scan

ABSTRACT

Bimetallic (Pt and Cu) nanoparticles (NPs) were homogeneously deposited on graphene oxide (GO) sheets, by the hydrothermal reaction of H_2PtCl_6 and $Cu(NO_3)_2$ in the presence of GO. Transmission electron microscopy and X-ray photoelectron and Raman spectroscopies were used to characterize the surface morphology and structure of the GO/bimetallic NPs. Their nonlinear optical (NLO) and optical limiting (OL) properties were characterized by open-aperture Z-scan measurements, using a 532-nm laser with a pulse duration of ~4 ns. The GO/bimetallic NPs exhibited enhanced NLO and OL properties, compared with GO and GO coated with single-metal NPs. The two-photon absorption of GO sheets, nonlinear scattering of Pt and Cu NPs, inter-band transition of Pt and Cu NPs, and charge transfer between GO and metal NPs all contributed to the enhanced NLO and OL properties of the GO/Pt–Cu NPs. The GO/bimetallic NPs are promising candidates for optical limiters.

1. Introduction

Lasers were invented in 1960, and have been applied in energy weapons, optical communications, measurement, and chemical and materials preparation and processing. However, protecting sensitive optical devices and human eyes is important. Optical limiters (OLs) exhibit decreasing transmittance with increasing laser fluence, and can be used to protect eyes and sensitive optical devices from laser-induced damage. OL behavior has been observed in organic dyes (e.g., phthalocyanine and porphyrins) [1–3], carbon-based materials (e.g., carbon nanotubes, fullerenes, graphene) [4–6], metal and semiconductor nanoparticles (NPs) [7–9], and quantum dots [10–12]. Graphene has received much attention, because of its extended π-conjugated system and linear dispersion relationship of its electronic band structure. Graphene exhibits strong OL properties, so can be used in broad-band limiters. Its OL properties largely originate from nonlinear scattering (NLS), reverse saturable absorption (RSA), two-photon absorption (TPA), and multi-photon absorption [13–18].

Graphene oxide (GO) is a chemically exfoliated graphene derivative. GO is easily modified and functionalized through abundant oxygen-containing functional groups at its surface and edges. GO and GO-based materials have attracted much attention, because of their useful electronic, optical, mechanical, and chemical properties. They have potential applications in high-performance electronic, catalytic, and sensing devices [19,20]. Nanocomposites based on graphene and its derivatives, including functionalized graphene hybrids, exhibit improved nonlinear optical (NLO) and OL properties, compared with their corresponding single components. Thus, various studies have investigated graphene-based hybrids as optical limiters [21–25].

Anchoring noble metal nanoparticles (NPs) such as Au, Ag, Pt, and Pd on the surface of graphene has attracted considerable interest [26–28]. Such metal NPs are easily prepared, easily dispersed, and stable in aqueous and organic solvents, and exhibit OL properties and ultra-fast response times. Oxygen-containing groups within GO can act as nucleation sites for nanostructure growth, and promote the formation of metal NPs. This promotes the formation of well-dispersed metal NPs on graphene hybrid materials. Several studies have investigated these composite materials [26–28]. The OL efficiency of functionalized hydrogen-exfoliated graphene was improved upon the infusion of Pt and Pd NPs. This was because of increased nonlinear absorption (NLA), originating from inter-band transition and charge transfer [26]. The TPA emission of GO-Au nanocrystal composites was significantly enhanced, compared with that of Au nanocrystals [27]. Most reports on the OL effects of graphene coated with metal NPs have focused on single-metal NPs. Coating GO with bimetallic NPs has received little attention, despite such composites exhibiting enhanced catalytic activity [29]. Understanding the NLO and OL behaviors of graphene coated with bimetallic NPs will promote the application of GO-metal nanocomposites in nonlinear optics.

* Corresponding author. Tel.: +86 591 22863279.
E-mail address: czheng.fjut@gmail.com (C. Zheng).

http://dx.doi.org/10.1016/j.ijleo.2015.11.094
0030-4026/

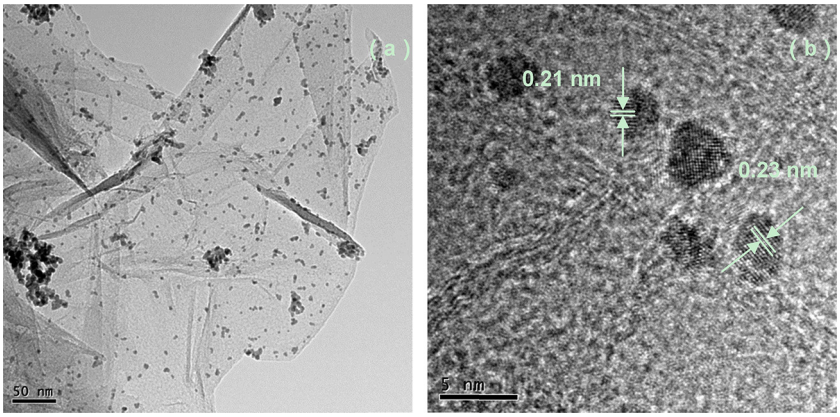

Fig. 1. Typical TEM images of GO/Pt–Cu NPs.

Herein, Pt and Cu NPs are homogeneously deposited on GO sheets to yield GO/Pt–Cu NPs. Transmission electron microscopy (TEM), X-ray photoelectron spectroscopy (XPS), and Raman spectroscopy are used to characterize the surface morphology and structure of the GO/metal NPs. The NLO and OL properties of the GO/metal NPs are characterized by open-aperture (OA) Z-scan measurements, using a 532-nm laser with a pulse duration of ~4 ns. The GO/metal NPs exhibit enhanced NLO and OL properties, compared with those of GO. The mechanisms for this enhancement are discussed.

2. Experimental

2.1. Synthesis of materials

2.1.1. Synthesis of GO

Graphene was prepared by oxidizing natural graphite powder via the modified Hummers' method [30]. Approximately 10 g of graphite powder and 5 g of sodium nitrate were simultaneously stirred in concentrated sulfuric acid (230 mL), while cooling in an ice bath. Thirty grams of potassium permanganate was gradually added. The mixture was allowed to warm to room temperature, heated to 35 °C in a water bath, and then gently stirred for 2 h. The reaction mixture was then cooled in an ice bath, and excess distilled water was added. Aqueous hydrogen peroxide (30 wt.%) was added, and the mixture was stirred for 2 h to reduce excess $KMnO_4$. The resulting suspension was thoroughly washed with dilute HCl and distilled water, via filtration. The suspension was centrifuged at 3000 rpm, to remove residual unexfoliated graphite and oxidant. The resulting material was lyophilized to obtain GO powder.

2.1.2. Synthesis of GO/bimetallic NPs

GO (15 mg) was dispersed in ethylene glycol (45 mL) by ultrasonication for 1 h. The solution was then stirred and heated to 170 °C. Aqueous $H_2PtCl_6{\cdot}6H_2O$ (15 mL, 4.0 mM) and $Cu(NO_3)_2{\cdot}3H_2O$ (15 mL, 4.0 mM) were added as precursors, and the pH was adjusted to ~7 with aqueous NaOH. The mixture was kept at 170 °C for 20 min. The resulting nanocomposite was washed with distilled water, and centrifuged (3000 rpm) to remove free Pt and Cu NPs formed in solution. The GO/Pt–Cu NPs were then lyophilized. GO/Pt NPs were similarly prepared, except in the absence of $Cu(NO_3)_2{\cdot}3H_2O$.

2.2. Characterization

The morphology of the GO/bimetallic NPs was investigated using TEM (JEM-2010, JEOL Ltd., Japan) at an accelerating voltage of 200 kV. Samples were first ultrasonically dispersed in ethanol, a drop of which was allowed to dry on a commercial carbon-coated Cu TEM grid. XPS was performed using an Escalab 250 spectrometer (Thermo Fisher Scientific Inc., MA, USA) with an Al K_α radiation excitation source. Binding energies were calibrated using the C1s peak at 285 eV, when samples exhibited mild charging. Raman spectra of GO and the GO/Pt–Cu NPs were obtained using a Raman spectrometer (Renishaw Invia, Gloucestershire, UK), at ambient temperature with a 785-nm excitation wavelength.

2.3. Z-scan measurements

The NLO and OL behaviors of GO and the GO/bimetallic NPs were evaluated from OA Z-scan measurements [31]. The excitation source was a Nd:YAG laser (Brio 640, Quantel, Les Ulis, France), with a repetition rate of 1 Hz. The 532-nm laser pulses (4-ns period) were split into two beams by a mirror. The pulse energies at the front and back of the samples were monitored using D1 and D2 energy detectors (PE25; Ophir Optronics Solutions Ltd., Jerusalem, Israel). The laser beam waist was approximately 14.5 μm, and the energy of a single pulse was 200 μJ. All measurements were conducted at room temperature. Samples were dispersed in ethanol and transferred into 1-mm-thick glass cuvettes. Each sample was mounted on a computer-controlled translation stage, which shifted the sample along the *z*-axis.

3. Results and discussion

3.1. Morphology and structure of the GO/Pt–Cu NPs

The morphology of the GO/Pt–Cu NPs was investigated by TEM. Fig. 1(a) shows that the GO/Pt–Cu NPs have a sheet-like morphology, with some corrugations. Many ultrafine Pt and Cu NPs are homogenously dispersed on the GO sheets. The HRTEM image shown in Fig. 1(b) provides information about the particle size and crystal lattice. Two well-defined lattice spacings of ~0.23 and ~0.21 nm correspond to the (1 1 1) planes of Pt and Cu, respectively. The Pt and Cu particle sizes are ~3–4 nm. Several larger clusters are observed in Fig. 1(a), indicating the aggregation of Pt and Cu NPs. Smaller particles are more prone to aggregation, especially on the nanoscale. Ultrafine and uniformly dispersed Pt and Cu NPs are therefore obtained from the hydrothermal reaction of H_2PtCl_6 and $Cu(NO_3)_2{\cdot}3H_2O$ in the presence of GO.

XPS was used to investigate the surface composition and chemical states in the GO/Pt–Cu NPs. Fig. 2(a) shows the XPS survey scan of the GO/Pt–Cu NPs, in which C, O, Pt, and Cu are detected. The Pt 4f spectral region is shown in Fig. 2(b), and two obvious peaks are observed. No other peaks can be deconvoluted. Thus, the hydrothermal reaction reduced H_2PtCl_6 into its metallic state. The